

On Stereo Viewing of SAR Images

FRANZ W. LEBERL, SENIOR MEMBER, IEEE, JOHANNES RAGGAM, AND MICHAEL KOBRICK, MEMBER, IEEE

Abstract—The interpretability of side-looking radar images can be significantly enhanced by the use of overlapping image strips viewed stereoscopically. Although the subject has been studied for many years, the lack of systematically acquired data has meant that the optimum sensor geometry for good stereo viewing and mapping accuracy is still undetermined. This paper attempts to evaluate stereo viewability using available real images and describes on-going work utilizing digital elevation maps and computer image simulation.

I. INTRODUCTION

STEREO viewing of overlapping images is a valuable tool in photointerpretation. It is also indispensable for the identification and measurement of homologue points in two overlapping images and subsequent reconstruction of the three-dimensional topographic relief. This may serve to create a model of terrain topography, e.g., in the form of contours, or to selectively measure slopes and relative height differences. The emphasis in this contribution is on viewing of radar data and on subjective visual impressions. It is not on the accuracy of reconstructing three-dimensional coordinates.

"Stereo" derives from the greek word *stereos* (hard, solid). The perception of space with two eyes is often called natural binocular vision. Stereo viewing refers to a visual perception of space by presenting an overlapping image pair to an observer so that a three-dimensional model is formed in the brain. The machine-correlation of two overlapping images can be called "automated stereo correlation."

This terminology is based on the authoritative review of LaPrade *et al.* [16]. It differs from that used for example in the german photogrammetric literature (Rinner and Burkhardt [22]) where both the direct perception of space and the viewing of overlapping images are denoted by stereo viewing. Techniques of generating three-dimensional object space coordinates from sets of monocular-image measurements is the topic of stereology.

For the observer, radar-stereo viewing is hardly different from viewing conventional photographs, although there exists an entirely different projection geometry and mathematical model. The human observer perceives displacements of image points due to height differences (relief displacement). These form so-called parallax differences irrespective of whether we

deal with natural binocular vision or with two images in stereoscopic viewing.

Already, a considerable body of literature has accumulated on stereo radar, beginning with LaPrade [13]. Previous work was reviewed and some numerical results were presented by Leberl [20]. Stereo viewability of radar images was discussed by LaPrade [14], Graham [9], Leberl [18], [19], [20] and by Kaupp *et al.* [11]. Computation of three-dimensional object coordinates from overlapping images was analyzed by Innes [10], Rosenfield [23], Gracie *et al.* [8], Konecny [12], DBA-Systems [4], Goodyear [7], Derenyi [5], and Leberl [17]–[19].

The most commonly discussed radar stereo imaging arrangements have either both flights to the same side or each of the two flights at opposite sides of the object. Other arrangements have been described but have not materialized; these include cross-wise flights (Graham [9]), and different flight altitudes, or single flight convergent schemes such as with tilted antennas in a real aperture radar (Leberl [17], Carlson [3], and Bair and Carlson [1], [2]). It is not possible to generate stereo SAR from a single straight flight line, a topic discussed in a preceding study (Leberl [20]).

The current paper follows previous theoretical error analyses. Based on this work, image pairs are evaluated using the concept of exaggeration factors. The data permit us to draw preliminary conclusions on the viewability of stereo radar and some simulated radar images support these preliminary conclusions. Viewable stereo with maximum exaggeration is obtained with intersection angles of up to 60°.

II. STEREO VIEWING GEOMETRY

A. General

The minimum observable retinal disparity for binocular vision is reported by LaPrade *et al.* [16] at 3". Muenster [21] reports a mean value of 6", found under good lighting conditions. The optimum can be achieved with lines in object space that run parallel. On the other hand, there exists also a maximum viewable-stereo disparity angle; this amounts to 70" (Rinner and Burkhardt [22]). Monocularly, two objects can be distinguished if they create an angular disparity in one eye of perhaps 20". Thus stereoscopy has a distinct advantage: if one were to monocularly measure the same point in two images, a measuring error will be committed that is several times larger than in a stereoscopic mode. Measurements in overlapping images should, therefore, always be made stereoscopically.

B. Stereo Evaluation with an Exaggeration Factor

Stereo-imaging geometry is usually being judged by two numbers. The first, $1/t$, indicates a ratio between a parallaxic

Manuscript received January 18, 1983; revised December 7, 1983. A modified version of this paper was presented at IGARSS 1982, Munich, Germany, June 1–4, 1982, under the title "Stereo Side-Looking Radar Experiments." F. Leberl and J. Raggam were supported by the Austrian Ministry of Science and Research, under Research Contract 6.931/3–27/1980. This work was carried out in part by the Jet Propulsion Laboratory, California Institute of Technology, under contract with NASA.

F. Leberl and J. Raggam are with the Technical University and Graz Research Center, A-8010 Graz, Austria.

M. Kobrick is with the Jet Propulsion Laboratory, California Institute of Technology, Pasadena, CA 91109.

distance obtained by natural binocular vision and the parallax distance observed in the stereoscopic-image pair; t is called the "total plastic." It is assumed that natural vision and stereo-image generation are from the same distance to the object. Typically, t can be as large as several hundred thousand. Since the figure compares natural binocular vision with stereoscopic images it is not of interest in the current context.

The second number is of greater significance; it describes the "flatness" of the observed stereoscopic impression in the form of an "exaggeration factor" q . Since we observe stereo imagery with a central perspective geometry, we need first to understand this factor for that arrangement, then extend the concept to apply to radar-image geometry as well. Stereoscopic exaggeration, or affine stretch, of the observed object is a common concept that is discussed in photogrammetric manuals (LaPrade *et al.* [16], Rinner and Burkhardt [22]). For ease of reference, we present this concept.

Fig. 1 shows the central perspective-image collection geometry for a pair of cameras and an observer looking at a stereoscopic image pair through the lenses of a stereoscope. The object is a pyramid of the height h_n and base w_n . For the exaggeration factor one defines the ratio h_n/w_n of the pyramid in object space. This appears from the stereo observation as h_s/w_s . This allows one to define q the exaggeration factor q as a measure of the flatness of the observed stereo model

$$q = (h_s/w_s)/(h_n/w_n). \quad (1)$$

It can be shown that the exaggeration factor is independent of the dimensions of the object and merely depends on the so-called "base:height ratios," H_n/B_n in object space, and H_s/B_s for stereo viewing

$$q = (H_s/B_s)/(B_n/H_n). \quad (2)$$

The transformation of (1) into (2) is discussed by LaPrade *et al.* [16].

In natural binocular vision the eyes form a convergence angle γ of about 14° or less and convert to a value for H_s/B_s of about 4 or larger. Experimental work of LaPrade [15] supports the conclusion that optimum stereoscopic viewing is achieved with a value that is about 5, so that

$$q = 5(B_n/H_n). \quad (3)$$

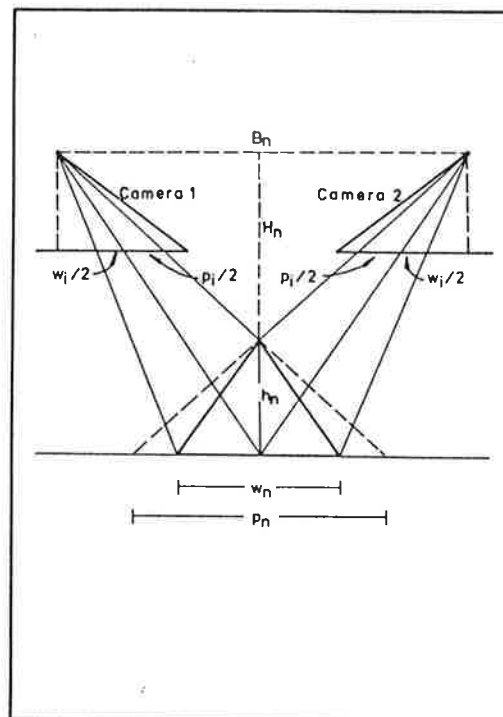
This stereo-exaggeration factor will be subsequently applied to radar images.

III. RADAR STEREOSCOPY

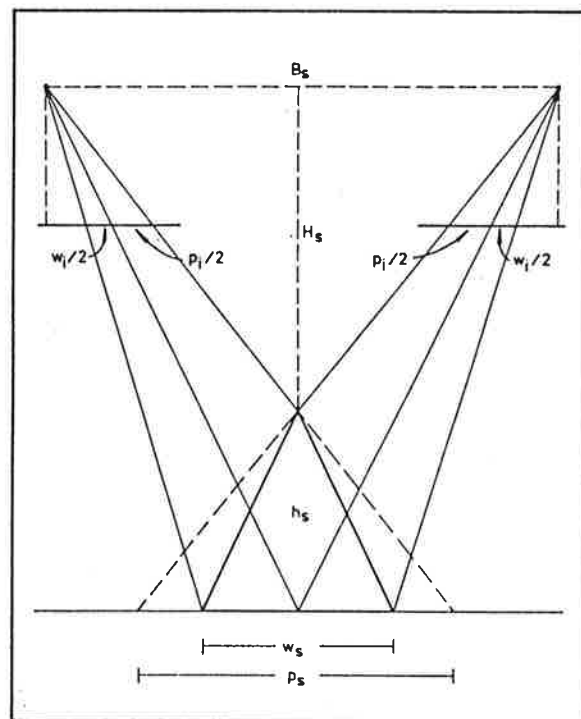
A. Viewability of Real Images

The two partners of a stereo-image pair must be very similar in image quality or thematic content (tone, texture, etc.) so that they correlate well, whereas they should be sufficiently different in geometry to present parallaxes for height perception. Since radar is actively illuminating the target, differences in geometry due to different sensor positions imply illumination differences also.

From a geometric point of view, good stereo, therefore, seems to conflict with good viewability. In aerial photo



(a)



(b)

Fig. 1. Definitions for the vertical-exaggeration factor after LaPrade *et al.* [16]. (a) Object space; (b) in stereoscopic viewing.

interpretation the required parallaxes are obtained without any illumination differences in the two stereo partners; the sun illumination hardly changes from one photograph to the next. Stereo viewability is not a problem with photography. It is the essential problem with radar. Figs. 2-8 present some examples of stereo-radar models from:

- 1) aircraft with opposite-side illumination (Fig. 2);

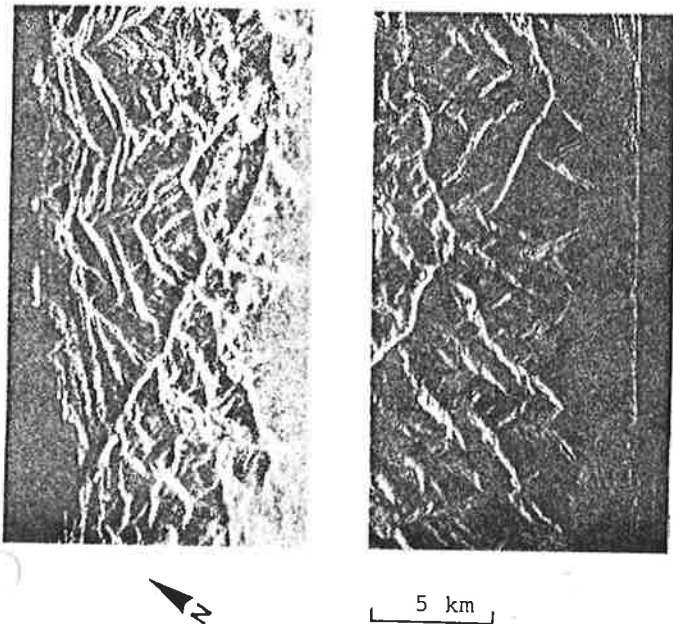


Fig. 2. Opposite-side stereo with aircraft radar, 25-cm wavelength (Jet Propulsion Laboratory); 10-km flying height. Edge of Grand Canyon, AZ.

- 2) aircraft, with same-side illumination (Figs. 3 and 4);
- 3) same-side illumination from an aircraft and satellite SAR (Figs. 4 and 5);
- 4) satellite (Seasat) with same-side and opposite-side illumination (Figs. 6 and 7); and
- 5) lunar Apollo 17 radar with same-side illumination (Fig. 8).

Table I reviews a set of stereo configurations, including those shown here, with a subjective evaluation of viewability by an observer. The conclusion from the study of a larger set of radar stereo pairs confirms earlier findings (Leberl [20]). Influencing factors on stereo are stereo arrangement, look angles off-nadir, stereo intersection angles, and ruggedness of the imaged area.

Viewability is thus ensured at shallow look angles for same-side arrangements. Opposite-side stereo may be feasible with flat or gently rolling terrain. The limits of the actual performance cannot be defined precisely using imagery available today. One has to investigate this with the help of an even larger set of images, in particular with a larger variety of cases; image simulation offers a means to evaluate the subjective capability of an observer viewing radar stereo data.

LaPrade [15] reports on one experiment with operators studying same-side stereo of flat areas with man-made objects. Optimum results were reported to require look angles of 37° – 67° off-nadir and intersection angles of about 12° – 15° . These intersection angles may seem poor, but it will be shown later that radar has the potential to still produce vertical-exaggeration factors approaching those of standard photo-interpretation.

B. Radar Stereoscopic Computations

General formulations for radar-stereo computations have been proposed by Gracie *et al.* [8] and others. The literature

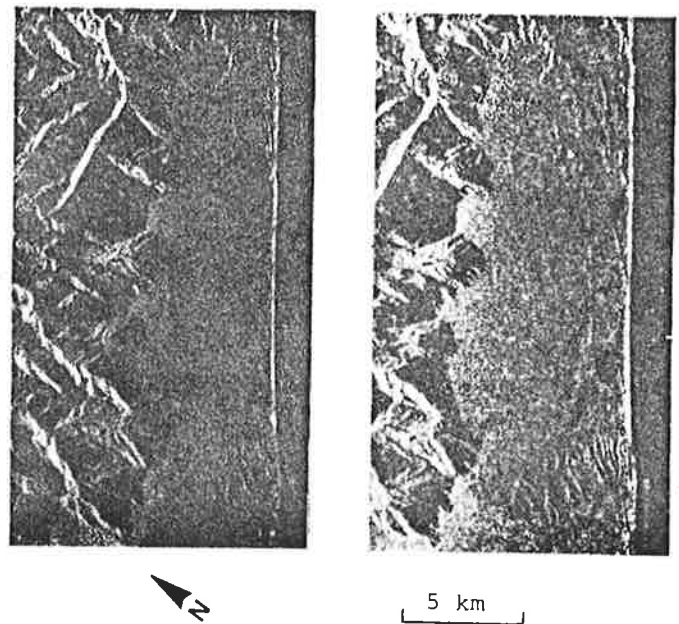


Fig. 3. Same-side stereo with aircraft radar, same as Fig. 2.

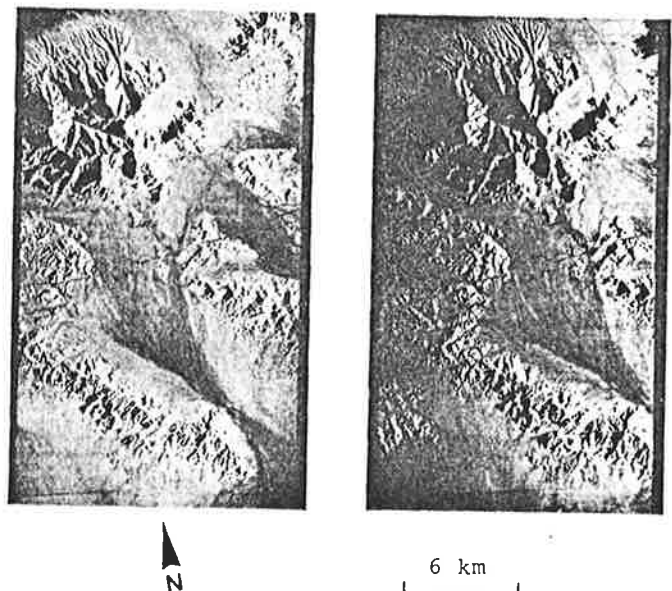


Fig. 4. Same-side stereo with aircraft radar Granite Mountain, AZ, 12-km altitude, (courtesy Goodyear-Aeroservice).

was reviewed by Leberl [20]. Simplified formulations are more commonly employed. For these, a rectilinear flight at constant altitude is assumed with the flight direction parallel to the object x coordinate axis (Fig. 9). We read from the figure that the object x_p, y_p, z_p coordinates of a point p are

$$\begin{aligned} x_p &= x_s \\ y_p &= (r'^2 - r''^2 + B^2)/(2B) \\ z_p &= H - ((r'^2 - y_p^2)^{1/2} + (r''^2 - (B - y_p)^2)^{1/2})/2 \end{aligned} \quad (4)$$

where B is the stereo base, H is the flying height.

A slightly different approach to compute the height h above a reference datum is still with projection circles

TABLE I
SUMMARY OF VIEWABILITY TEST FOR RADIO STEREO WITH ACTUAL IMAGERY

Type of Radar	Number of Models Studied	Base Length (km)	Look Angles (θ')	Type of Stereo	Intersection Angle $\Delta\theta$	Type of Terrain	Stereo Viewability
SEASAT	10	25 - 75	20°	Same-side	$10. - 40.8$	Rugged	very convenient
SAR	1	550	20°	Opposite s.	40°	Rugged	not possible
Aircraft SAR	4	0.7 - 13	68°	Same-side	$0^\circ.2 - 23^\circ$	Rugged	very convenient
Goodyear	2	30	68°	Opposite s.	120°	flat to rugged	only when flat
Aircraft Real Aperture	1	10	81°	Same-side	6°	flat to hilly	convenient
Motorola	1	48	80°	Opposite s.	160°	flat to hilly	only when flat
Lunar Apollo 17 ALSE-SAR	19	0.7 - 10.3	10°	Same-side	$0^\circ.3 - 5^\circ.3$	flat	convenient
						Rugged	only with $\Delta\theta \leq 1.9$

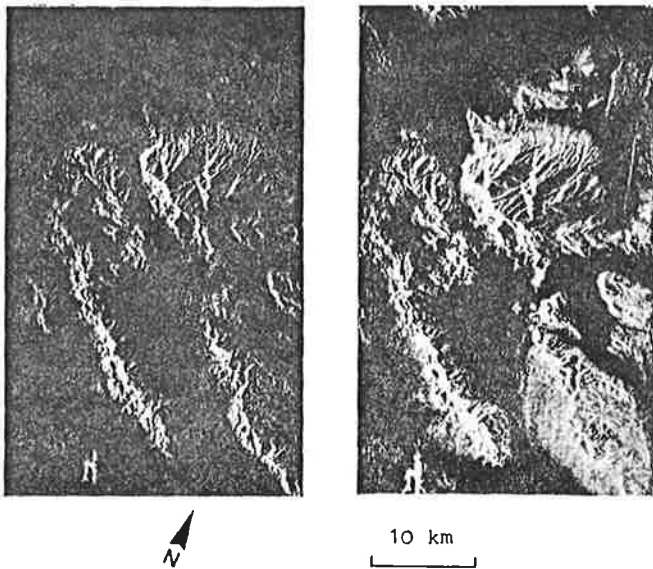


Fig. 5. Same area as Fig. 4. Seasat-SAR, 800-km altitude, 25-cm wavelength.

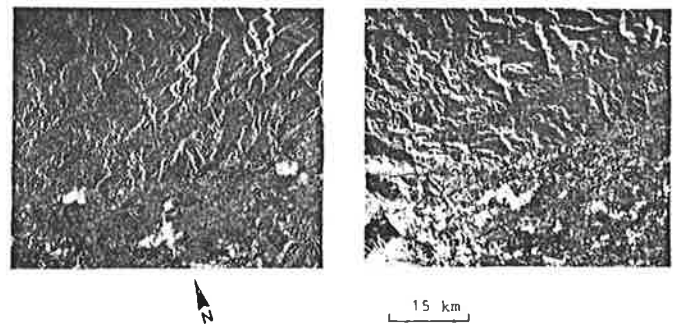


Fig. 7. Seasat-SAR opposite-side stereo of Los Angeles, CA. Partial overlap with area in Fig. 6.

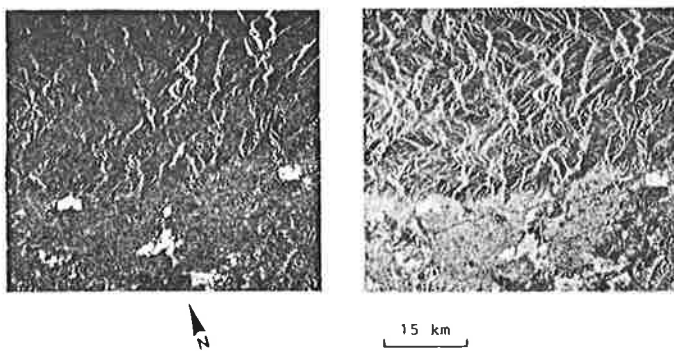


Fig. 6. Seasat-SAR same-side stereo of Los Angeles.

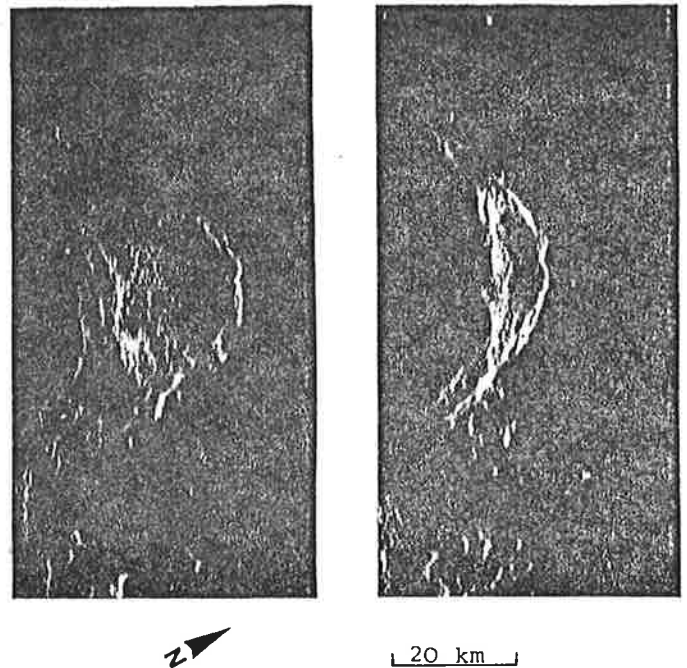


Fig. 8. Apollo 17-SAR of Buisson Crater on Moon, 116-km altitude, 2-m wavelength.

$$\begin{aligned}
 y_p &= \tan \theta'(H - h) \\
 y_p &= \pm \tan \theta''(H - h) + B \\
 z_p &= H - B / (\tan \theta' \pm \tan \theta'') \quad (5)
 \end{aligned}$$

range images, and with $z_p = h$

To relate the object height h above the reference datum to parallax difference d_p measured on an image pair for given look and intersection angles we have from Fig. 9 for ground-

$$p'_g = (H - h) \tan \theta' - ((H - h)^2 / \cos^2 \theta' - H^2)^{1/2}.$$

This converts to

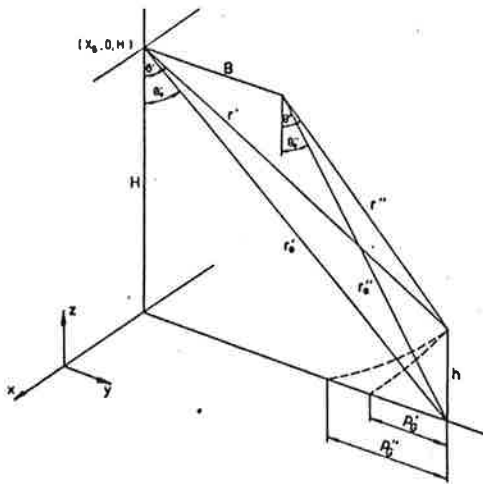


Fig. 9. Definition of entities for stereo-radar images.

$$p' = (H - h) \tan \theta' - (1 + h^2/(H^2 \sin^2 \theta')) - 2h/(H \sin^2 \theta') H \tan \theta'. \quad (6a)$$

Similarly we find for the other image

$$p'' = (H - h) \tan \theta'' - (1 + h^2/(H^2 \sin^2 \theta'')) - 2h/(H \sin^2 \theta'') H \tan \theta''. \quad (6b)$$

We define

$$d_{pg} = p'' - p'. \quad (6c)$$

In order to obtain an algebraically explicit expression for d_{pg}/h we neglect the expression with h in the second bracket of (6a) and (6b) assuming that h/H is small and θ' is not small. We then obtain

$$d_{pg}/h = \tan \theta'' - \tan \theta'. \quad (6d)$$

Note that a given parallax d_{pg} generates a different height h depending on θ' and θ'' . This means that apparent heights will change across a stereo model, in contrast to photographic stereo where a given parallax corresponds to the same height independent of where in the stereo model it has been observed. Note also that the neglect made to obtain an algebraic expression for d_{pg}/h is acceptable only if θ' , θ'' are not small.

For slant-range images, parallax difference can be defined as follows:

$$d_{ps} = r'' - r' = (H - h) (\sec \theta'' - \sec \theta').$$

Here, unlike ground-range pairs, we find that zero heights still generate nonzero parallaxes. This means that the datum surface in a slant-range pair will appear curved, which we may calculate by setting $h = 0$, $\theta' = \theta'_0$ and $\theta'' = \theta''_0$

$$d_p \text{ datum} = H(\sec \theta''_0 - \sec \theta'_0).$$

Topographic relief will appear to lie on top of this curved surface, according to

$$d_{ps} - d_p \text{ datum} = (H - h) (\sec \theta'' - \sec \theta') - H(\sec \theta''_0 - \sec \theta'_0). \quad (7)$$

We also know that

$$\tan \theta' = y/(H - h) \quad \tan \theta'' = (y - B)/(H - h)$$

$$\tan \theta'_0 = y/H \quad \tan \theta''_0 = (y - B)/H.$$

These combine to yield

$$\sec \theta' = (1 + \tan^2 \theta'_0 \cdot H^2/(H - h)^2)^{1/2}$$

$$\sec \theta'' = (1 + \tan^2 \theta''_0 \cdot H^2/(H - h)^2)^{1/2}.$$

Substituting in (7)

$$\begin{aligned} (d_{ps} - d_p \text{ datum})/h &= [((H - h)^2 + H^2 \tan^2 \theta''_0)^{1/2} \\ &\quad - ((H - h)^2 + H^2 \tan^2 \theta'_0)^{1/2} \\ &\quad - H \cdot (\sec \theta''_0 - \sec \theta'_0)]/h. \end{aligned} \quad (8a)$$

If we assume that h^2/H^2 is small and can be neglected, then we obtain

$$\begin{aligned} (d_{ps} - d_p \text{ datum})/h &= ((\sec^2 \theta''_0 - 2h/H)^{1/2} - (\sec^2 \theta'_0 - 2h/H)^{1/2} \\ &\quad - \sec \theta'_0 + \sec \theta'_0) H/h. \end{aligned} \quad (8b)$$

Equations (6) and (8) allow one to compute parallax differences for each stereo configuration and object-height difference, and will be used for the evaluation of exaggeration factors in the following section.

IV. DEFINITION OF RADAR STEREOSCOPIC EXAGGERATION

The exaggeration factor q as defined for camera photography relates a subjectively observed pyramid in the stereoscopic model to the same pyramid in object space. Since we can relate the radar stereo parallax d_p to the equivalent photographic stereo case it is possible to compare the quality of the radar and camera stereoscopic impressions. We merely need to find the photographic base: height ratio, B_n/H_n , of a fictitious camera arrangement that would produce the same parallax d_p obtained from radar for a given object height h . The exaggeration factor q is formed from (3).

In the case of a camera, we take B_n/H_n from

$$B_n/H_n = d_{pn}/h_n. \quad (9)$$

Therefore

$$q = 5d_{pn}/h_n.$$

The ratio d_p/h needs to be found for radar. Using (6d) we find for ground-range images and θ values that are not small

$$q_g \approx 5(\tan \theta' - \tan \theta''). \quad (10)$$

For slant-range images we may use (8b) for the excess parallax of topography above the datum plane

$$\begin{aligned} q_s \approx & ((\sec^2 \theta''_0 - 2h/H)^{1/2} - (\sec^2 \theta'_0 - 2h/H)^{1/2} \\ & - \sec \theta''_0 + \sec \theta'_0) 5H/h. \end{aligned} \quad (11)$$

Table II has been computed using (6), (8), (10), and (11). We see in Table II that radar-stereo parallaxes and exaggeration factors compare well with values obtained from cameras: as look angles become steeper, one has a more accentuated stereo

TABLE I
EXAGGERATION FACTORS FOR RADAR-STEREO MODELS, GROUND AND
SLANT RANGE REPRESENTATIONS

Type of Radar	Stereo Base km	Look Angle θ' ($^\circ$)	Intersection Angle $\Delta\theta'$ ($^\circ$)	Flying Height H (km)	Parallax Diff. due to h=1km Ground ranges	Exaggeration Factors	
						Ground Ranges qs	Slant Ranges qs
SEASAT	25	20	1.6	800	0.263	1.3	0.05
	75	22	4.8	800	0.761	3.8	0.14
Aircraft SAR	0.7	68	0.5	12	0.011	0.06	0.04
	13.5	65	23	12	0.720	3.6	1.60
Goodyear Aircraft RAR	10	81	10	4	0.215	1.1	0.95
	48	80	160	4	0.414	2.1	2.01
Motorola	0.7	10	0.3	116	0.383	1.9	0.00
Apollo 17	3.9	10	1.9	116	3.422	17.1	0.03
ALSE	10.0	13	4.7	116	2.584	12.9	0.07
Moon	10.0	13	4.8	116	5.220	26.1	0.08

TABLE II
ROOT-MEAN-SQUARE ERRORS OF RADARGRAMMETRIC HEIGHTS AFTER
POLYNOMIAL CORRECTION WITH 17 COEFFICIENTS
(Aircraft radar is the Goodyear Electronic Mapping System.)

Imagery	Measurement	Nr. of measured points	R.m.s. height error (m)
Seasat, Granite Mtn. Optical	Parallax bar stereo plotter	28	96
		28	121
Aircraft, Granite Mtn. Optical	Parallax bar stereo plotter	21	49
		21	48
Seasat, L.A. Digital	Parallax bar	28	143
Seasat, L.A. Optical		28	121

effect in spite of small stereo-intersection angles. This assumes extreme values for a case such as Apollo 17-ALSE, where very small intersection angles create parallaxes that are multiples of the object height. In camera photogrammetry, the largest parallaxes are of the order of an observed height difference, as q values range between 3 and 5.

Factor q results from a deterministic model of radar stereo parallaxes and addresses the question of an affine stretch of the stereo model. Large exaggeration factors result from large parallaxes but do not ensure high accuracy of coordinate measurements. The discussion excludes error propagation into measurements of base width B_n and of parallaxes d_p . Theoretical error considerations were presented by Leberl [20]. In the case of ALSE radar the vertical exaggeration is extreme, the reconstruction of the three-dimensional coordinates is not of increasing accuracy as q increases. In the limiting case of an altimeter, the vertical accuracy would be good only at the expense of a degenerating horizontal coordinate measuring capability.

V. IMAGE SIMULATION

Simulated radar images can be used to evaluate stereo-radar viewing. We have experimented with a simulation procedure based on digital elevation models (DEM's) to serve as a tool for radar-image rectification and radiometric analysis. A

separate paper describes the technique and first application (Domik *et al.* [6]). Radar-image pairs from DEM's of the area around Mt. Shasta in Northern California and in other areas have shown that stereo viewing is feasible in all same-side cases with orbital-radar images, even with intersection angles of up to 60° . Difficulties exist only when excessive layover (at 10° look angles) is combined with shadows (80° look angle). No useful opposite-side stereo was found even with a broad range of simulated data.

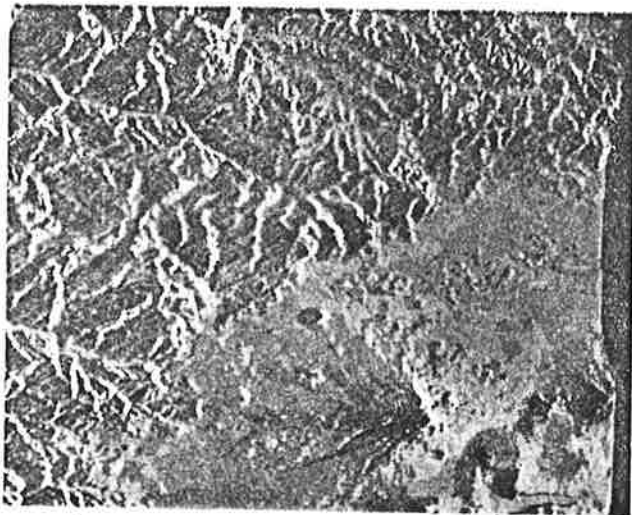
No real radar images exist today to confirm this result. Fig. 10 is an example of simulated radar stereo pairs of Mt. Shasta.

The conclusions essentially confirm the published results of Kaupp *et al.* [11] with the difference that Kaupp *et al.* find optimum stereo angles of 40° - 45° . Additional studies will have to address more quantitatively the many detailed effects of influencing factors on stereo viewing and measurement accuracy.

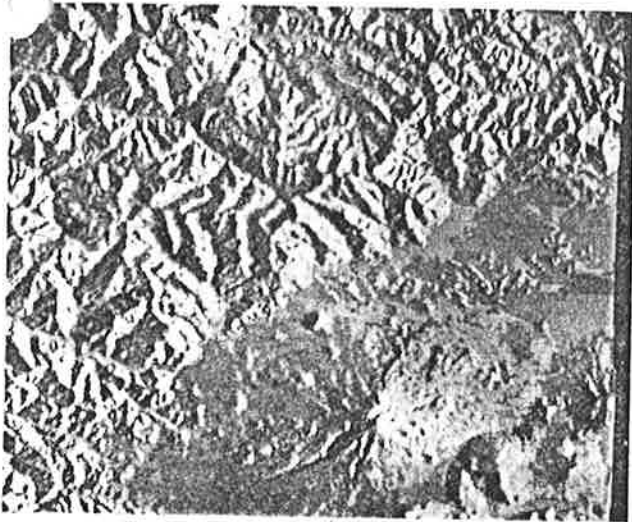
VI. ACCURACY WITH PARALLAX MEASUREMENTS IN RADAR IMAGES

As a by-product of the stereo-viewing evaluation, height measurement accuracies were obtained from a number of radar-image pairs as presented in Table III.

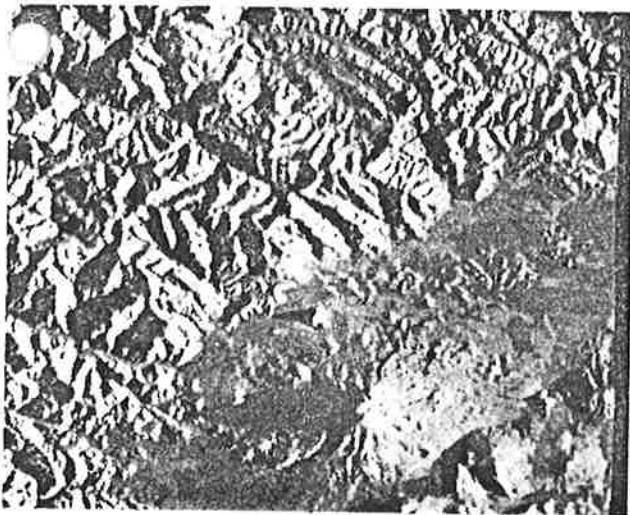
Parallax measurements were taken in two ways: with a stereoscope and parallax bar, and with a conventional photo



(a)



(b)



(c)

Fig. 10. Three simulated radar images with Seasat-SAR geometry of Mt. Shasta, USA. (a) $\theta = 20^\circ$, (b) $\theta = 60^\circ$, and (c) $\theta = 80^\circ$.

grammetric plotter used as a comparator. All images are of the same-side type.

Six radar-stereo models were observed; height differences

d_h were computed at control points between known heights h and radar-derived heights h' . These discrepancies were used to define a correction polynomial and final radar heights h' as

$$h' = \bar{h}' + \sum_{i=1}^3 \sum_{j=1}^3 a_{ij} x^{(i-1)} y^{(j-1)}. \quad (12)$$

Table III presents the results of this exercise in the form of root-mean-square residuals. The following conclusions result:

- 1) the stereoplotter was not superior to simple parallax bar measurements;
- 2) systematic errors exist in all raw heights and need to be corrected with the use of control points and correction polynomials;
- 3) aircraft radar provided higher accuracies than Seasat, although differences are not distinct;
- 4) satellite radar of Los Angeles is poorer than of Granite Mountains because of a smaller stereo base; and
- 5) digital and optical correlations led to the same performance figures with the images that were employed.

VII. CONCLUSIONS AND OUTLOOK

An evaluation with a large set of about 40 radar stereo models demonstrates that same-side arrangements provide good stereo viewability; this was confirmed for aircraft radar with look angles off-nadir of 60° - 80° and intersection angles between 0.2° and 23° , and for satellite radar (Seasat) with look angles of 20° and intersection angles of 1.2° - 4.8° . In the case of extremely steep illumination such as in the Apollo 17-ALSE radar on the Moon, same-side stereo of mountainous areas was impossible when the intersection angles were in excess of about 2° . Look angles were around 0° - 10° degrees in that project. No other radar stereo was available at the time of the study. Stereo viewability at other look and intersection angles needs to be explored with simulated radar images.

Height accuracies in same-side aircraft radar of mountainous terrain amounted to 50 m after a 17-parameter polynomial correction. Satellite radar from Seasat was somewhat inferior with errors in excess of 100 m for the same areas and same type of correction polynomial. Again this concerns currently available stereo cases with their inherent limitations.

Vertical-exaggeration factors were computed in Table II and serve to describe the flatness of the observed stereo model, relating the presentation of height to that of planimetric dimensions. These factors were between 0.06 and 3.6 for aircraft, between 1.3 and 3.8 for available Seasat data and between 1.9 and 26 for Apollo-17 data. This compares with a value of $q = 3$ -5 for standard aircraft wide-angle photography. We see for the very small intersection angles of satellite radar that the vertical exaggeration factors are rather large. This, however, is valid due to the small look angles off-nadir where small intersection angles still create large parallaxes in ground-range presentations. It does not imply high geometric accuracy of coordinate measurements.

Further work needs to address in more detail the effect of a wide range of radar-stereo arrangements on viewability, accuracy, and exaggeration factors; this will require a more complete set of images covering wider ranges of parameters. A

useful approach is through image simulation, from which a limited result was obtained in the current study, indicating that same-side stereo is viewable nearly in all cases, even with intersection angles of 60° .

The extent to which nonparallel flight lines can still lead to valid radar stereo imagery is of interest in satellite radar. This will be a topic of experimentation in the Shuttle Imaging Radar (SIR-B) and can be based on some limited data from the SIR-A experiment.

REFERENCES

- [1] G. L. Bair and G. E. Carlson, "Height measurement with stereo radar," *Photogramm. Eng.*, vol. XLI, 1975.
- [2] —, "Performance comparison of techniques for obtaining stereo radar images," *IEEE Trans. Geosci. Electron.*, vol. GE-11, 1974.
- [3] G. E. Carlson, "An improved single-flight technique for radar stereo," *IEEE Trans. Geosci. Electron.*, vol. GE-11, no. 4, 1973.
- [4] "Research studies and investigations for radar control extensions," DBA Systems, Incorporated, Melbourne, FL, Defense Documentation Center Rep. 530784L, 1974.
- [5] E. E. Derenyi, "Topographical accuracy of side looking radar imagery," *Bildmessung und Luftbildwesen*, no. 1, 1975.
- [6] G. Domik, M. Kobrick, and F. Leberl, "Radarbildanalyse mit digitalen Höhenmodellen," *Bildmessung und Luftbildwesen*, no. 5, pp. 249-263, 1984.
- [7] "Preliminary imagery data analysis Goodyear electronic mapping system (GEMS)," Goodyear Aerospace Corporation, Rep. GIB-9342, Code 99696, 1974.
- [8] G. Gracie *et al.*, "Stereo radar analysis," US Engineer Topographic Laboratory, Ft. Belvoir, VA, Rep. FTR-1339-1, 1970.
- [9] L. Graham, "Flight planning for radar stereo mapping," in *Proc. Am. Soc. Photogramm., 41st Meeting* (Washington, DC), 1975.
- [10] R. B. Innes, "Principles of SLAR-measurements of the third coordinate of target position," Project Michigan, Rep. 2900-474-T, 1964.
- [11] V. Kaupp, L. Bridges, M. Pizaruck, H. MacDonald, and W. Waite, "Comparison of simulated stereo radar imagery," presented at IGARSS 1982, Munich, FRG, Paper TA4, Jun. 1-4, 1982.
- [12] G. Konecny, "Geometrische Probleme der Fernerkundung," *Bildmessung und Luftbildwesen*, vol. 42, no. 2, 1972.
- [13] G. L. LaPrade, "An analytical and experimental study of stereo for radar," *Photogramm. Eng.*, vol. XXIX, 1963.
- [14] —, "Subjective considerations for stereo radar," Goodyear Aerospace Corporation, Rep. GIB-9169, and also in *Photogramm. Eng.*, 1970.
- [15] —, "Addendum to GIB-9169, subjective considerations for stereo radar," Goodyear Aerospace Corporation, AZ, 1975.
- [16] G. L. LaPrade *et al.*, "Stereoscopy," in *Manual of Photogrammetry*, 4th ed, Falls Church, VA: Amer. Soc. Photogramm., 1980.
- [17] F. Leberl, "On model formation with remote sensing imagery," *Osterreichische Z. für Vermessungswesen*, Nov. 2, 1972.
- [18] —, "Lunar radargrammetry with ALSE-VHF-Imagery," in *Proc. Amer. Soc. Photogramm.*, Phoenix, AZ, Fall 1975.
- [19] —, "Satellitenradargrammetrie," Deutsche Geodaetische Kommission, Series C, no. 239, Munich, Germany, 1978, p. 156.
- [20] —, "Accuracy aspects of stereo-side-looking radar," JPL Publ. 79-17, Jet Propulsion Laboratory, Pasadena, CA, 1979.
- [21] C. Muenster, "Ueber einige Probleme der stereoskopischen Messung," *Z. für Instrumentenkunde*, pp. 346-357, 1942.
- [22] K. Rinner and R. Burkhardt, "Photogrammetrie," Band III a/1, *Handbuch der Vermessungskunde*. Stuttgart, Germany: J. B. Metzler'sche Verlagsbuchhandlung, 1972.
- [23] G. H. Rosenfield, "Stereo Radar Techniques," *Photogramm. Eng.*, vol. XXXIV, 1968.



Franz W. Leberl (SM'82) was born in 1945. He received the Dipl.Ing. degree in geodetic engineering in 1967 and the Dr.Tech. degree in 1972, both from the Technical University, Vienna, Austria.

He has worked at the International Institute for Aerial Surveys and Earth Sciences, Delft and Enschede, the Netherlands, from 1969 to 1974. From 1974 to 1976, he was a research associate at the Jet Propulsion Laboratory, Pasadena, CA. From 1976 to 1984, he held an appointment at the Technical University, Graz, Austria, as a Professor of Photogrammetry and Remote Sensing. Simultaneously, he was Director of the Research Institute for Image Processing and Computer Graphics, Graz Research Center, Graz, Austria. He currently works with Markhurd Corporation, Minneapolis, MN. He has authored about 100 articles.

Dr. Leberl was recipient of the Otto von Gruber Gold Medal of the International Society for Photogrammetry and Remote Sensing in 1976.

Michael Kobrick (M'81) received the B.S. degree in physics from Rensselaer Polytechnic Institute, Troy, NY, the M.S. degree in astronomy from the University of Illinois and the M.S. and Ph.D. degree in planetary and space science from the University of California, Los Angeles.

A Research Scientist at the Jet Propulsion Laboratory, Pasadena, CA, his current research interests include radar remote sensing of planetary surfaces and, in particular, the derivation and geophysical analysis of topographic information. He is the Science Manager of the Venus Radar Mapper project, a Principal Investigator on the Shuttle Imaging Radar, Coinvestigator in the development of a new high-frequency radar altimeter for the Mars Geoscience and Climatology Orbiter, and Principal Investigator of the Digital Topographic Mapping Mission study project.

Dr. Kobrick is a member of the American Astronomical Society, Divisions for Planetary Science and Dynamical Astronomy, American Geophysical Union, AAAS, Sigma Xi American Institute of Physics, Astronomical Society of the Pacific, and the American Society of Photogrammetry, and has served on several NASA advisory panels for planetary radar as well as the Federal Interagency Coordinating Committee for Digital Cartography.



Johannes Raggam received the Dipl.Ing. degree in geodetic engineering from the Technical University, Graz, Austria, in 1980. He is currently working toward the Ph.D. degree on the subject of stereo radar at the Research Institute for Image Processing and Computer Graphics of the Graz Research Center, Graz, Austria.

As part of his work, he developed a capability to employ a photogrammetric computer controlled stereo instrument with overlapping side-looking radar images.

On Stereo Viewing of SAR Images

FRANZ W. LEBERL, SENIOR MEMBER, IEEE, JOHANNES RAGGAM, AND MICHAEL KOBRICK, MEMBER, IEEE

Abstract—The interpretability of side-looking radar images can be significantly enhanced by the use of overlapping image strips viewed stereoscopically. Although the subject has been studied for many years, the lack of systematically acquired data has meant that the optimum sensor geometry for good stereo viewing and mapping accuracy is still undetermined. This paper attempts to evaluate stereo viewability using available real images and describes on-going work utilizing digital elevation maps and computer image simulation.

I. INTRODUCTION

STEREO viewing of overlapping images is a valuable tool in photointerpretation. It is also indispensable for the identification and measurement of homologous points in two overlapping images and subsequent reconstruction of the three-dimensional topographic relief. This may serve to create a model of terrain topography, e.g., in the form of contours, or to selectively measure slopes and relative height differences. The emphasis in this contribution is on viewing of radar data and on subjective visual impressions. It is not on the accuracy of reconstructing three-dimensional coordinates.

"Stereo" derives from the greek word *stereos* (hard, solid). The perception of space with two eyes is often called natural binocular vision. Stereo viewing refers to a visual perception of space by presenting an overlapping image pair to an observer so that a three-dimensional model is formed in the brain. The machine-correlation of two overlapping images can be called "automated stereo correlation."

This terminology is based on the authoritative review of LaPrade *et al.* [16]. It differs from that used for example in the german photogrammetric literature (Rinner and Burkhardt [22]) where both the direct perception of space and the viewing of overlapping images are denoted by stereo viewing. Techniques of generating three-dimensional object space coordinates from sets of monocular-image measurements is the topic of stereology.

For the observer, radar-stereo viewing is hardly different from viewing conventional photographs, although there exists an entirely different projection geometry and mathematical model. The human observer perceives displacements of image points due to height differences (relief displacement). These form so-called parallax differences irrespective of whether we

deal with natural binocular vision or with two images in stereoscopic viewing.

Already, a considerable body of literature has accumulated on stereo radar, beginning with LaPrade [13]. Previous work was reviewed and some numerical results were presented by Leberl [20]. Stereo viewability of radar images was discussed by LaPrade [14], Graham [9], Leberl [18], [19], [20] and by Kaupp *et al.* [11]. Computation of three-dimensional object coordinates from overlapping images was analyzed by Innes [10], Rosenfield [23], Gracie *et al.* [8], Konecny [12], DBA-Systems [4], Goodyear [7], Derenyi [5], and Leberl [17]-[19].

The most commonly discussed radar stereo imaging arrangements have either both flights to the same side or each of the two flights at opposite sides of the object. Other arrangements have been described but have not materialized; these include cross-wise flights (Graham [9]), and different flight altitudes, or single flight convergent schemes such as with tilted antennas in a real aperture radar (Leberl [17], Carlson [3], and Bair and Carlson [1], [2]). It is not possible to generate stereo SAR from a single straight flight line, a topic discussed in a preceding study (Leberl [20]).

The current paper follows previous theoretical error analyses. Based on this work, image pairs are evaluated using the concept of exaggeration factors. The data permit us to draw preliminary conclusions on the viewability of stereo radar and some simulated radar images support these preliminary conclusions. Viewable stereo with maximum exaggeration is obtained with intersection angles of up to 60°.

II. STEREO VIEWING GEOMETRY

A. General

The minimum observable retinal disparity for binocular vision is reported by LaPrade *et al.* [16] at 3". Muenster [21] reports a mean value of 6", found under good lighting conditions. The optimum can be achieved with lines in object space that run parallel. On the other hand, there exists also a maximum viewable-stereo disparity angle; this amounts to 70" (Rinner and Burkhardt [22]). Monocularly, two objects can be distinguished if they create an angular disparity in one eye of perhaps 20". Thus stereoscopy has a distinct advantage: if one were to monocularly measure the same point in two images, a measuring error will be committed that is several times larger than in a stereoscopic mode. Measurements in overlapping images should, therefore, always be made stereoscopically.

B. Stereo Evaluation with an Exaggeration Factor

Stereo-imaging geometry is usually being judged by two numbers. The first, $1/t$, indicates a ratio between a parallaxic

Manuscript received January 18, 1983; revised December 7, 1983. A modified version of this paper was presented at IGARSS 1982, Munich, Germany, June 1-4, 1982, under the title "Stereo Side-Looking Radar Experiments." F. Leberl and J. Raggam were supported by the Austrian Ministry of Science and Research, under Research Contract 6.931/3-27/1980. This work was carried out in part by the Jet Propulsion Laboratory, California Institute of Technology, under contract with NASA.

F. Leberl and J. Raggam are with the Technical University and Graz Research Center, A-8010 Graz, Austria.

M. Kobrick is with the Jet Propulsion Laboratory, California Institute of Technology, Pasadena, CA 91109.

distance obtained by natural binocular vision and the parallax distance observed in the stereoscopic-image pair; t is called the "total plastic." It is assumed that natural vision and stereo-image generation are from the same distance to the object. Typically, t can be as large as several hundred thousand. Since the figure compares natural binocular vision with stereoscopic images it is not of interest in the current context.

The second number is of greater significance; it describes the "flatness" of the observed stereoscopic impression in the form of an "exaggeration factor" q . Since we observe stereo imagery with a central perspective geometry, we need first to understand this factor for that arrangement, then extend the concept to apply to radar-image geometry as well. Stereoscopic exaggeration, or affine stretch, of the observed object is a common concept that is discussed in photogrammetric manuals (LaPrade *et al.* [16], Rinner and Burkhardt [22]). For ease of reference, we present this concept.

Fig. 1 shows the central perspective-image collection geometry for a pair of cameras and an observer looking at a stereoscopic image pair through the lenses of a stereoscope. The object is a pyramid of the height h_n and base w_n . For the exaggeration factor one defines the ratio h_n/w_n of the pyramid in object space. This appears from the stereo observation as h_s/w_s . This allows one to define q the exaggeration factor q as a measure of the flatness of the observed stereo model

$$q = (h_s/w_s)/(h_n/w_n). \quad (1)$$

It can be shown that the exaggeration factor is independent of the dimensions of the object and merely depends on the so-called "base:height ratios," H_n/B_n in object space, and H_s/B_s for stereo viewing

$$q = (H_s/B_s)/(B_n/H_n). \quad (2)$$

The transformation of (1) into (2) is discussed by LaPrade *et al.* [16].

In natural binocular vision the eyes form a convergence angle γ of about 14° or less and convert to a value for H_s/B_s of about 4 or larger. Experimental work of LaPrade [15] supports the conclusion that optimum stereoscopic viewing is achieved with a value that is about 5, so that

$$q = 5(B_n/H_n). \quad (3)$$

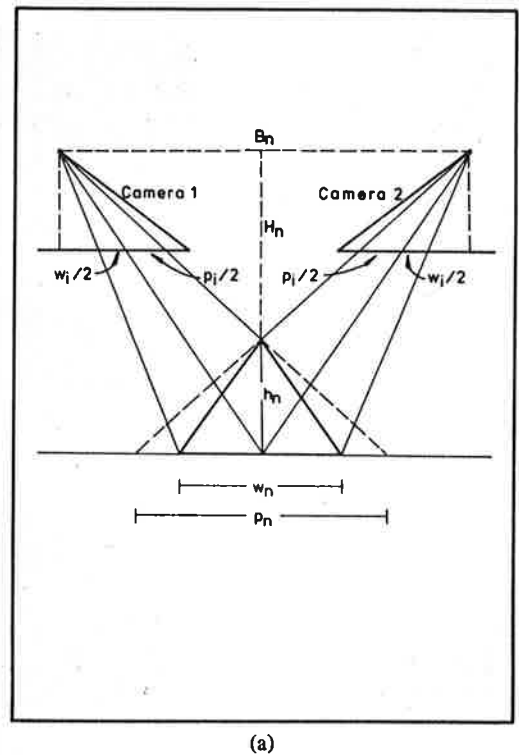
This stereo-exaggeration factor will be subsequently applied to radar images.

III. RADAR STEREOCOPY

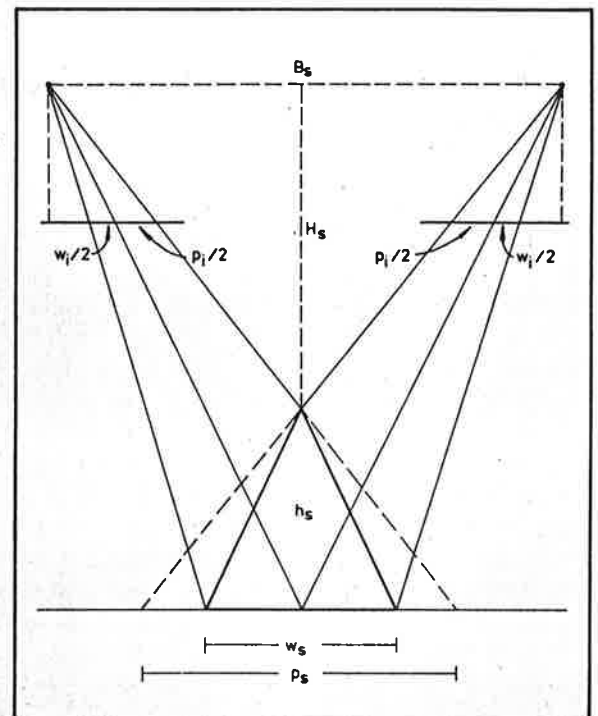
A. Viewability of Real Images

The two partners of a stereo-image pair must be very similar in image quality or thematic content (tone, texture, etc.) so that they correlate well, whereas they should be sufficiently different in geometry to present parallaxes for height perception. Since radar is actively illuminating the target, differences in geometry due to different sensor positions imply illumination differences also.

From a geometric point of view, good stereo, therefore, seems to conflict with good viewability. In aerial photo



(a)



(b)

Fig. 1. Definitions for the vertical-exaggeration factor after LaPrade *et al.* [16]. (a) Object space; (b) in stereoscopic viewing.

interpretation the required parallaxes are obtained without any illumination differences in the two stereo partners; the sun illumination hardly changes from one photograph to the next. Stereo viewability is not a problem with photography. It is the essential problem with radar. Figs. 2-8 present some examples of stereo-radar models from:

- 1) aircraft with opposite-side illumination (Fig. 2);

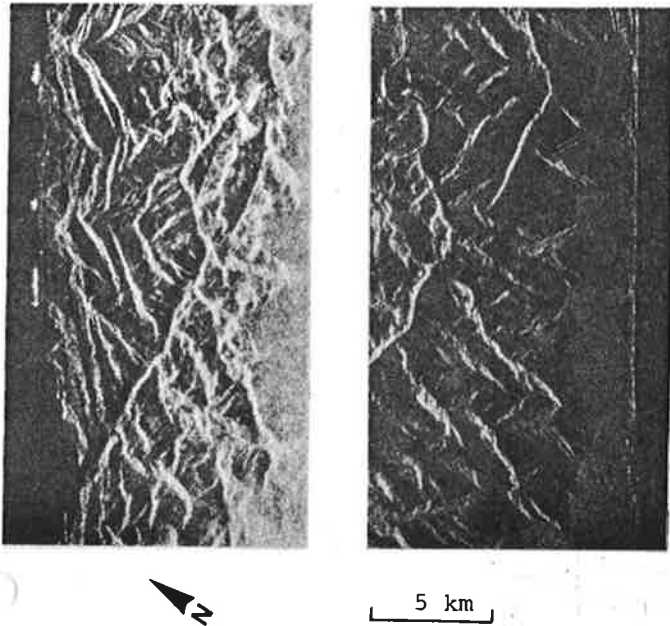


Fig. 2. Opposite-side stereo with aircraft radar, 25-cm wavelength (Jet Propulsion Laboratory); 10-km flying height. Edge of Grand Canyon, AZ.

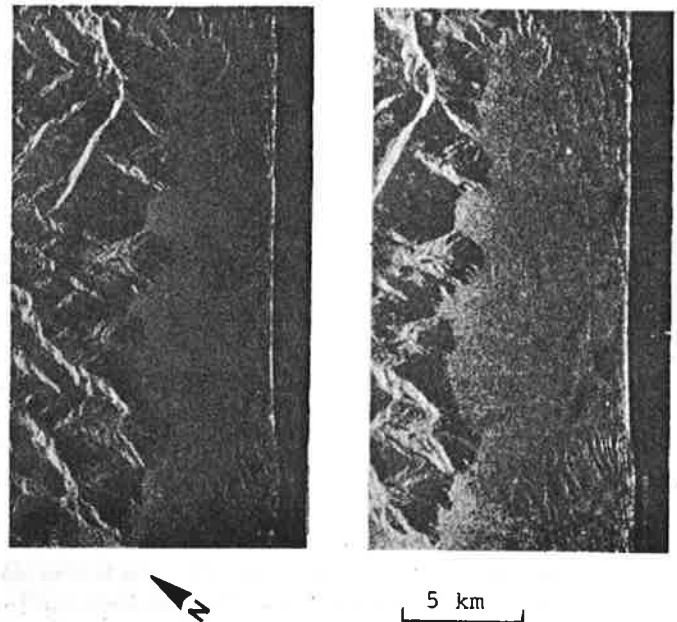


Fig. 3. Same-side stereo with aircraft radar, same as Fig. 2.

- 2) aircraft, with same-side illumination (Figs. 3 and 4);
- 3) same-side illumination from an aircraft and satellite SAR (Figs. 4 and 5);
- 4) satellite (Seasat) with same-side and opposite-side illumination (Figs. 6 and 7); and
- 5) lunar Apollo 17 radar with same-side illumination (Fig. 8).

Table I reviews a set of stereo configurations, including those shown here, with a subjective evaluation of viewability by an observer. The conclusion from the study of a larger set of radar stereo pairs confirms earlier findings (Leberl [20]). Influencing factors on stereo are stereo arrangement, look angles off-nadir, stereo intersection angles, and ruggedness of the imaged area.

Viewability is thus ensured at shallow look angles for same-side arrangements. Opposite-side stereo may be feasible with flat or gently rolling terrain. The limits of the actual performance cannot be defined precisely using imagery available today. One has to investigate this with the help of an even larger set of images, in particular with a larger variety of cases; image simulation offers a means to evaluate the subjective capability of an observer viewing radar stereo data.

LaPrade [15] reports on one experiment with operators studying same-side stereo of flat areas with man-made objects. Optimum results were reported to require look angles of 37° – 67° off-nadir and intersection angles of about 12° – 15° . These intersection angles may seem poor, but it will be shown later that radar has the potential to still produce vertical-exaggeration factors approaching those of standard photo-interpretation.

B. Radar Stereoscopic Computations

General formulations for radar-stereo computations have been proposed by Gracie *et al.* [8] and others. The literature

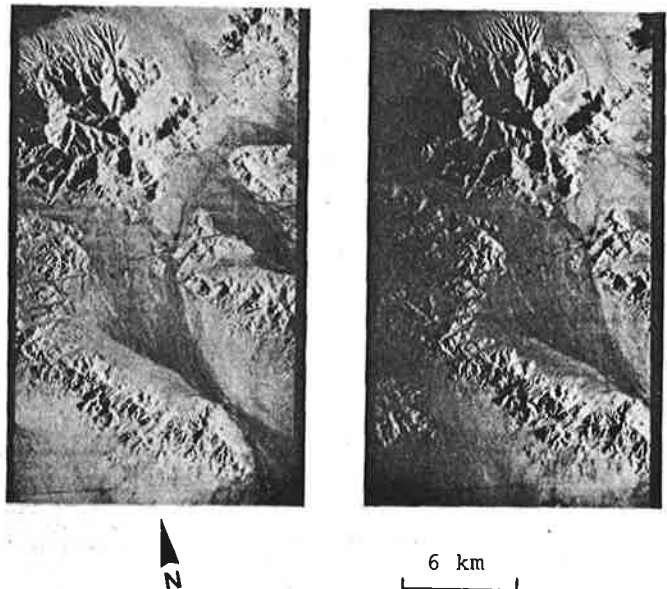


Fig. 4. Same-side stereo with aircraft radar Granite Mountain, AZ, 12-km altitude, (courtesy Goodyear-Aeroservice).

was reviewed by Leberl [20]. Simplified formulations are more commonly employed. For these, a rectilinear flight at constant altitude is assumed with the flight direction parallel to the object x coordinate axis (Fig. 9). We read from the figure that the object x_p, y_p, z_p coordinates of a point p are

$$\begin{aligned} x_p &= x_s \\ y_p &= (r'^2 - r''^2 + B^2)/(2B) \\ z_p &= H - ((r'^2 - y_p^2)^{1/2} + (r''^2 - (B - y_p)^2)^{1/2})/2 \end{aligned} \quad (4)$$

where B is the stereo base, H is the flying height.

A slightly different approach to compute the height h above a reference datum is still with projection circles

TABLE I
SUMMARY OF VIEWABILITY TEST FOR RADIO STEREO WITH ACTUAL IMAGERY

Type of Radar	Number of Models Studied	Base Length (km)	Look Angles θ'	Type of Stereo	Intersection Angle $\Delta\theta$	Type of Terrain	Stereo Viewability
SEASAT SAR	10	25 - 75	20°	Same-side	10°-40.8	Rugged	very convenient
	1	550	20°	Opposite s.	40°	Rugged	not possible
Aircraft SAR Goodyear	4	0.7 - 13	68°	Same-side	0°-2-23°	Rugged	very convenient
	2	30	68°	Opposite s.	120°	flat to rugged	only when flat
Aircraft Real Aperture Motorola	1	10	81°	Same-side	6°	flat to hilly	convenient
	1	48	80°	Opposite s.	160°	flat to hilly	only when flat
Lunar Apollo 17 ALSE-SAR	19	0.7 - 10.3	10°	Same-side	00.3-5°-3	flat	convenient
						Rugged	only with $\Delta\theta \leq 1.9$

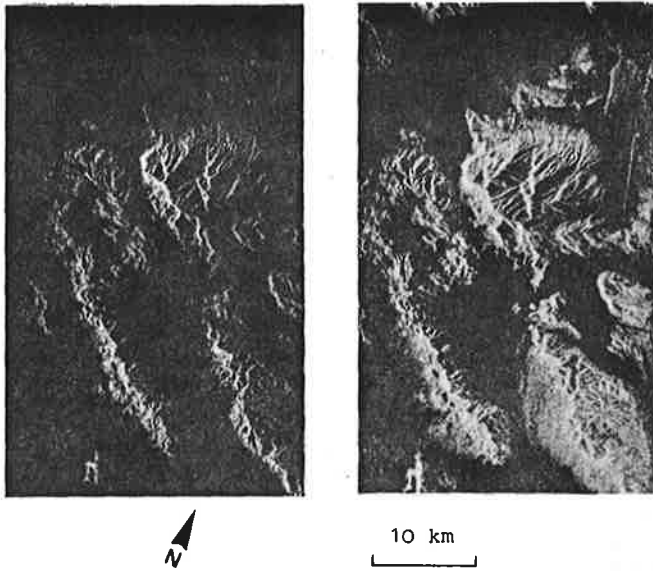


Fig. 5. Same area as Fig. 4. Seasat-SAR, 800-km altitude, 25-cm wavelength.

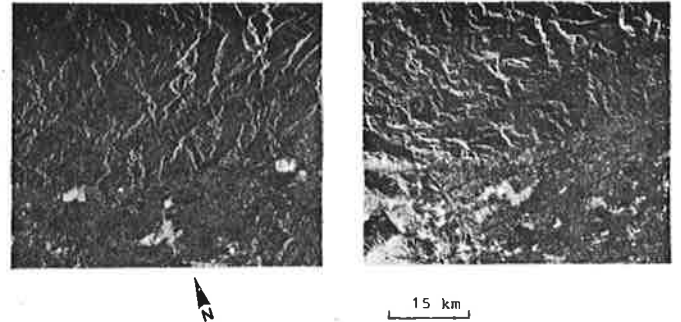


Fig. 7. Seasat-SAR opposite-side stereo of Los Angeles, CA. Partial overlap with area in Fig. 6.

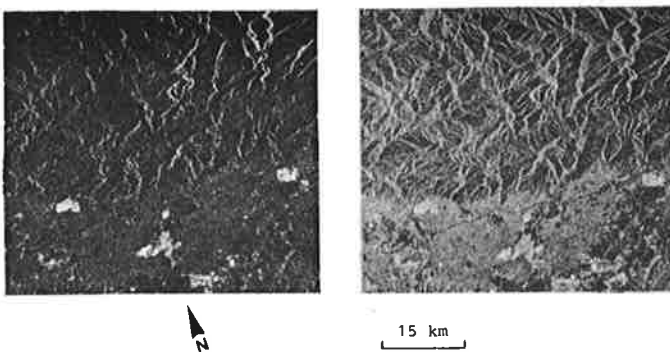


Fig. 6. Seasat-SAR same-side stereo of Los Angeles.

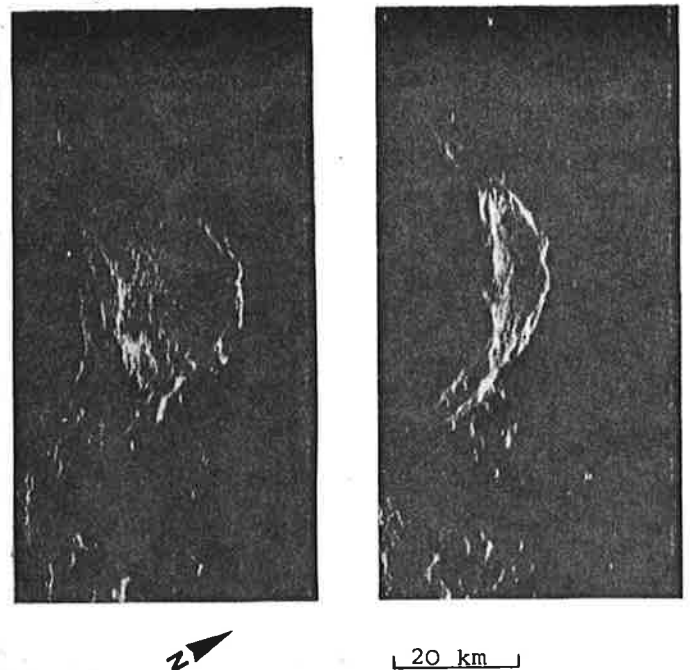


Fig. 8. Apollo 17-SAR of Buisson Crater on Moon, 116-km altitude, 2-m wavelength.

$$\begin{aligned}
 y_p &= \tan \theta'(H - h) \\
 y_p &= \pm \tan \theta''(H - h) + B \\
 z_p &= H - B/(\tan \theta' \pm \tan \theta'')
 \end{aligned}
 \tag{5}$$

To relate the object height h above the reference datum to parallax difference d_p measured on an image pair for given look and intersection angles we have from Fig. 9 for ground-

range images, and with $z_p = h$

$$p'_g = (H - h) \tan \theta' - ((H - h)^2 / \cos^2 \theta' - H^2)^{1/2}.$$

This converts to

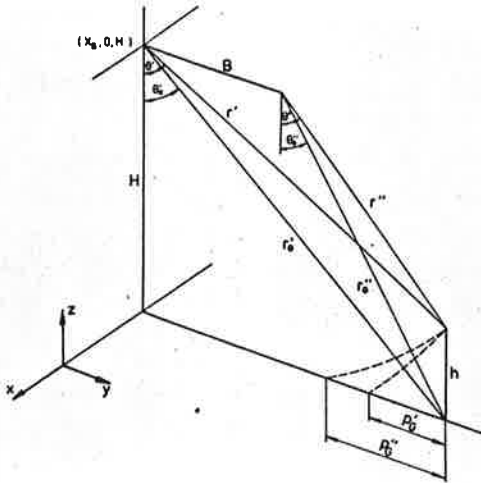


Fig. 9. Definition of entities for stereo-radar images.

$$p_g' = (H - h) \tan \theta' - (1 + h^2/(H^2 \sin^2 \theta')) \\ - 2h/(H \sin^2 \theta') H \tan \theta'. \quad (6a)$$

Similarly we find for the other image

$$p_g'' = (H - h) \tan \theta'' - (1 + h^2/(H^2 \sin^2 \theta'')) \\ - 2h/(H \sin^2 \theta'') H \tan \theta''. \quad (6b)$$

We define

$$d_{pg} = p_g'' - p_g'. \quad (6c)$$

In order to obtain an algebraically explicit expression for d_{pg}/h we neglect the expression with h in the second bracket of (6a) and (6b) assuming that h/H is small and θ' is not small. We then obtain

$$d_{pg}/h = \tan \theta'' - \tan \theta'. \quad (6d)$$

Note that a given parallax d_{pg} generates a different height h depending on θ' and θ'' . This means that apparent heights will change across a stereo model, in contrast to photographic stereo where a given parallax corresponds to the same height independent of where in the stereo model it has been observed. Note also that the neglect made to obtain an algebraic expression for d_{pg}/h is acceptable only if θ' , θ'' are not small.

For slant-range images, parallax difference can be defined as follows:

$$d_{ps} = r'' - r' \\ = (H - h) (\sec \theta'' - \sec \theta').$$

Here, unlike ground-range pairs, we find that zero heights still generate nonzero parallaxes. This means that the datum surface in a slant-range pair will appear curved, which we may calculate by setting $h = 0$, $\theta' = \theta'_0$ and $\theta'' = \theta''_0$

$$d_p \text{ datum} = H(\sec \theta''_0 - \sec \theta'_0).$$

Topographic relief will appear to lie on top of this curved surface, according to

$$d_{ps} - d_p \text{ datum} = (H - h) (\sec \theta'' - \sec \theta') \\ - H(\sec \theta''_0 - \sec \theta'_0). \quad (7)$$

We also know that

$$\tan \theta' = y/(H - H) \quad \tan \theta'' = (y - B)/(H - h)$$

$$\tan \theta'_0 = y/H \quad \tan \theta''_0 = (y - B)/H.$$

These combine to yield

$$\sec \theta' = (1 + \tan^2 \theta'_0 \cdot H^2/(H - h)^2)^{1/2}$$

$$\sec \theta'' = (1 + \tan^2 \theta''_0 \cdot H^2/(H - h)^2)^{1/2}.$$

Substituting in (7)

$$(d_{ps} - d_p \text{ datum})/h \\ = [((H - h)^2 + H^2 \tan^2 \theta''_0)^{1/2} \\ - ((H - h)^2 + H^2 \tan^2 \theta'_0)^{1/2} \\ - H \cdot (\sec \theta''_0 - \sec \theta'_0)]/h. \quad (8a)$$

If we assume that h^2/H^2 is small and can be neglected, then we obtain

$$(d_{ps} - d_p \text{ datum})/h \\ = ((\sec^2 \theta''_0 - 2h/H)^{1/2} - (\sec^2 \theta'_0 - 2h/H)^{1/2} \\ - \sec \theta'_0 + \sec \theta'_0) H/h. \quad (8b)$$

Equations (6) and (8) allow one to compute parallax differences for each stereo configuration and object-height difference, and will be used for the evaluation of exaggeration factors in the following section.

IV. DEFINITION OF RADAR STEREOSCOPIC EXAGGERATION

The exaggeration factor q as defined for camera photography relates a subjectively observed pyramid in the stereoscopic model to the same pyramid in object space. Since we can relate the radar stereo parallax d_p to the equivalent photographic stereo case it is possible to compare the quality of the radar and camera stereoscopic impressions. We merely need to find the photographic base: height ratio, B_n/H_n , of a fictitious camera arrangement that would produce the same parallax d_p obtained from radar for a given object height h . The exaggeration factor q is formed from (3).

In the case of a camera, we take B_n/H_n from

$$B_n/H_n = d_{pn}/h_n. \quad (9)$$

Therefore

$$q = 5d_{pn}/h_n.$$

The ratio d_p/h needs to be found for radar. Using (6d) we find for ground-range images and θ values that are not small

$$q_g \approx 5(\tan \theta' - \tan \theta''). \quad (10)$$

For slant-range images we may use (8b) for the excess parallax of topography above the datum plane

$$q_s \approx ((\sec^2 \theta''_0 - 2h/H)^{1/2} - (\sec^2 \theta'_0 - 2h/H)^{1/2} \\ - \sec \theta''_0 + \sec \theta'_0) 5H/h. \quad (11)$$

Table II has been computed using (6), (8), (10), and (11). We see in Table II that radar-stereo parallaxes and exaggeration factors compare well with values obtained from cameras: as look angles become steeper, one has a more accentuated stereo

TABLE I
EXAGGERATION FACTORS FOR RADAR-STEREO MODELS, GROUND AND
SLANT RANGE REPRESENTATIONS

Type of Radar	Stereo Base km	Look Angle θ' ($^\circ$)	Intersection Angle $\Delta\theta'$ ($^\circ$)	Flying Height H (km)	Parallax Diff. due to h=1km Ground ranges	Exaggeration Factors	
						Ground Ranges qg	Slant Ranges qs
SEASAT	25	20	1.6	800	0.263	1.3	0.05
	75	22	4.8	800	0.761	3.8	0.14
Aircraft SAR	0.7	68	0.5	12	0.011	0.06	0.04
	13.5	65	23	12	0.720	3.6	1.60
Goodyear Aircraft RAR	10	81	10	4	0.215	1.1	0.95
	48	80	160	4	0.414	2.1	2.01
Motorola	0.7	10	0.3	116	0.383	1.9	0.00
Apollo 17	3.9	10	1.9	116	3.422	17.1	0.03
ALSE	10.0	13	4.7	116	2.584	12.9	0.07
Moon	10.0	13	4.8	116	5.220	26.1	0.08

TABLE II
ROOT-MEAN-SQUARE ERRORS OF RADARGRAMMETRIC HEIGHTS AFTER
POLYNOMIAL CORRECTION WITH 17 COEFFICIENTS
(Aircraft radar is the Goodyear Electronic Mapping System.)

Imagery	Measurement	Nr. of measured points	R.m.s. height error (m)
Seasat, Granite Mtn. Optical	Parallax bar	28	96
	Stereo plotter	28	121
Aircraft, Granite Mtn. Optical	Parallax bar	21	49
	Stereo plotter	21	48
Seasat, L.A. Digital	Parallax bar	28	143
Seasat, L.A. Optical		28	121

effect in spite of small stereo-intersection angles. This assumes extreme values for a case such as Apollo 17-ALSE, where very small intersection angles create parallaxes that are multiples of the object height. In camera photogrammetry, the largest parallaxes are of the order of an observed height difference, as q values range between 3 and 5.

Factor q results from a deterministic model of radar stereo parallaxes and addresses the question of an affine stretch of the stereo model. Large exaggeration factors result from large parallaxes but do not ensure high accuracy of coordinate measurements. The discussion excludes error propagation into measurements of base width B_n and of parallaxes d_p . Theoretical error considerations were presented by Leberl [20]. In the case of ALSE radar the vertical exaggeration is extreme, the reconstruction of the three-dimensional coordinates is not of increasing accuracy as q increases. In the limiting case of an altimeter, the vertical accuracy would be good only at the expense of a degenerating horizontal coordinate measuring capability.

V. IMAGE SIMULATION

Simulated radar images can be used to evaluate stereo-radar viewing. We have experimented with a simulation procedure based on digital elevation models (DEM's) to serve as a tool for radar-image rectification and radiometric analysis. A

separate paper describes the technique and first application (Domik *et al.* [6]). Radar-image pairs from DEM's of the area around Mt. Shasta in Northern California and in other areas have shown that stereo viewing is feasible in all same-side cases with orbital-radar images, even with intersection angles of up to 60° . Difficulties exist only when excessive layover (at 10° look angles) is combined with shadows (80° look angle). No useful opposite-side stereo was found even with broad range of simulated data.

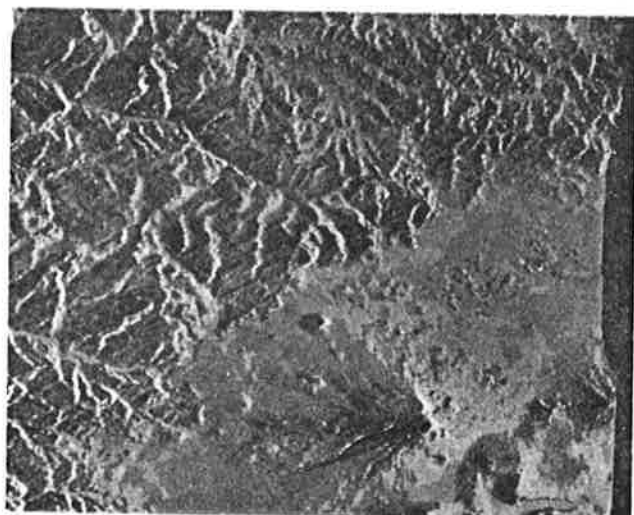
No real radar images exist today to confirm this result. Fig. 10 is an example of simulated radar stereo pairs of Mt. Shasta.

The conclusions essentially confirm the published results of Kaupp *et al.* [11] with the difference that Kaupp *et al.* find optimum stereo angles of 40° - 45° . Additional studies will have to address more quantitatively the many detailed effects of influencing factors on stereo viewing and measurement accuracy.

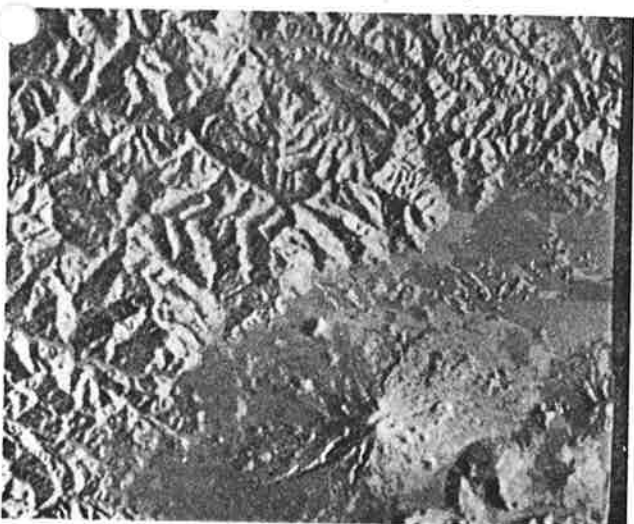
VI. ACCURACY WITH PARALLAX MEASUREMENTS IN RADAR IMAGES

As a by-product of the stereo-viewing evaluation, height measurement accuracies were obtained from a number of radar-image pairs as presented in Table III.

Parallax measurements were taken in two ways: with a stereoscope and parallax bar, and with a conventional photogrammetric



(a)



(b)



(c)

Fig. 10. Three simulated radar images with Seasat-SAR geometry of Mt. Shasta, USA. (a) $\theta = 20^\circ$, (b) $\theta = 60^\circ$, and (c) $\theta = 80^\circ$.

grammetric plotter used as a comparator. All images are of the same-side type.

Six radar-stereo models were observed; height differences

d_h were computed at control points between known heights h and radar-derived heights h' . These discrepancies were used to define a correction polynomial and final radar heights h' as

$$h' = \bar{h}' + \sum_{i=1}^3 \sum_{j=1}^3 a_{ij} x^{(i-1)} y^{(j-1)}. \quad (12)$$

Table III presents the results of this exercise in the form of root-mean-square residuals. The following conclusions result:

- 1) the stereoplotter was not superior to simple parallax bar measurements;
- 2) systematic errors exist in all raw heights and need to be corrected with the use of control points and correction polynomials;
- 3) aircraft radar provided higher accuracies than Seasat, although differences are not distinct;
- 4) satellite radar of Los Angeles is poorer than of Granite Mountains because of a smaller stereo base; and
- 5) digital and optical correlations led to the same performance figures with the images that were employed.

VII. CONCLUSIONS AND OUTLOOK

An evaluation with a large set of about 40 radar stereo models demonstrates that same-side arrangements provide good stereo viewability; this was confirmed for aircraft radar with look angles off-nadir of 60° - 80° and intersection angles between 0.2° and 23° , and for satellite radar (Seasat) with look angles of 20° and intersection angles of 1.2° - 4.8° . In the case of extremely steep illumination such as in the Apollo 17-ALSE radar on the Moon, same-side stereo of mountainous areas was impossible when the intersection angles were in excess of about 2° . Look angles were around 0° - 10° degrees in that project. No other radar stereo was available at the time of the study. Stereo viewability at other look and intersection angles needs to be explored with simulated radar images.

Height accuracies in same-side aircraft radar of mountainous terrain amounted to 50 m after a 17-parameter polynomial correction. Satellite radar from Seasat was somewhat inferior with errors in excess of 100 m for the same areas and same type of correction polynomial. Again this concerns currently available stereo cases with their inherent limitations.

Vertical-exaggeration factors were computed in Table II and serve to describe the flatness of the observed stereo model, relating the presentation of height to that of planimetric dimensions. These factors were between 0.06 and 3.6 for aircraft, between 1.3 and 3.8 for available Seasat data and between 1.9 and 26 for Apollo-17 data. This compares with a value of $q = 3$ -5 for standard aircraft wide-angle photography. We see for the very small intersection angles of satellite radar that the vertical exaggeration factors are rather large. This, however, is valid due to the small look angles off-nadir where small intersection angles still create large parallaxes in ground-range presentations. It does not imply high geometric accuracy of coordinate measurements.

Further work needs to address in more detail the effect of a wide range of radar-stereo arrangements on viewability, accuracy, and exaggeration factors; this will require a more complete set of images covering wider ranges of parameters. A

useful approach is through image simulation, from which a limited result was obtained in the current study, indicating that same-side stereo is viewable nearly in all cases, even with intersection angles of 60° .

The extent to which nonparallel flight lines can still lead to valid radar stereo imagery is of interest in satellite radar. This will be a topic of experimentation in the Shuttle Imaging Radar (SIR-B) and can be based on some limited data from the SIR-A experiment.

REFERENCES

- [1] G. L. Bair and G. E. Carlson, "Height measurement with stereo radar," *Photogramm. Eng.*, vol. XLI, 1975.
- [2] —, "Performance comparison of techniques for obtaining stereo radar images," *IEEE Trans. Geosci. Electron.*, vol. GE-11, 1974.
- [3] G. E. Carlson, "An improved single-flight technique for radar stereo," *IEEE Trans. Geosci. Electron.*, vol. GE-11, no. 4, 1973.
- [4] "Research studies and investigations for radar control extensions," DBA Systems, Incorporated, Melbourne, FL, Defense Documentation Center Rep. 530784L, 1974.
- [5] E. E. Derenyi, "Topographical accuracy of side looking radar imagery," *Bildmessung und Luftbildwesen*, no. 1, 1975.
- [6] G. Domik, M. Kobrick, and F. Leberl, "Radarbildanalyse mit digitalen Höhenmodellen," *Bildmessung und Luftbildwesen*, no. 5, pp. 249-263, 1984.
- [7] "Preliminary imagery data analysis Goodyear electronic mapping system (GEMS)," Goodyear Aerospace Corporation, Rep. GIB-9342, Code 99696, 1974.
- [8] G. Gracie *et al.*, "Stereo radar analysis," US Engineer Topographic Laboratory, Ft. Belvoir, VA, Rep. FTR-1339-1, 1970.
- [9] L. Graham, "Flight planning for radar stereo mapping," in *Proc. Am. Soc. Photogramm.*, 41st Meeting (Washington, DC), 1975.
- [10] R. B. Innes, "Principles of SLAR-measurements of the third coordinate of target position," Project Michigan, Rep. 2900-474-T, 1964.
- [11] V. Kaupp, L. Bridges, M. Pizaruck, H. MacDonald, and W. Waite, "Comparison of simulated stereo radar imagery," presented at IGARSS 1982, Munich, FRG, Paper TA4, Jun. 1-4, 1982.
- [12] G. Konecny, "Geometrische Probleme der Fernerkundung," *Bildmessung und Luftbildwesen*, vol. 42, no. 2, 1972.
- [13] G. L. LaPrade, "An analytical and experimental study of stereo for radar," *Photogramm. Eng.*, vol. XXIX, 1963.
- [14] —, "Subjective considerations for stereo radar," Goodyear Aerospace Corporation, Rep. GIB-9169, and also in *Photogramm. Eng.*, 1970.
- [15] —, "Addendum to GIB-9169, subjective considerations for stereo radar," Goodyear Aerospace Corporation, AZ, 1975.
- [16] G. L. LaPrade *et al.*, "Stereoscopy," in *Manual of Photogrammetry*, 4th ed, Falls Church, VA: Amer. Soc. Photogramm., 1980.
- [17] F. Leberl, "On model formation with remote sensing imagery," *Osterreichische Z. für Vermessungswesen*, Nov. 2, 1972.
- [18] —, "Lunar radargrammetry with ALSE-VHF-Imagery," in *Proc. Amer. Soc. Photogramm.*, Phoenix, AZ, Fall 1975.
- [19] —, "Satellitenradargrammetrie," Deutsche Geodaetische Kommission, Series C, no. 239, Munich, Germany, 1978, p. 156.
- [20] —, "Accuracy aspects of stereo-side-looking radar," JPL Publ. 79-17, Jet Propulsion Laboratory, Pasadena, CA, 1979.
- [21] C. Muenster, "Ueber einige Probleme der stereoskopischen Messung," *Z. für Instrumentenkunde*, pp. 346-357, 1942.
- [22] K. Rinner and R. Burkhardt, "Photogrammetrie," Band III a/1, *Handbuch der Vermessungskunde*. Stuttgart, Germany: J. B. Metzler'sche Verlagsbuchhandlung, 1972.
- [23] G. H. Rosenfield, "Stereo Radar Techniques," *Photogramm. Eng.*, vol. XXXIV, 1968.



Franz W. Leberl (SM'82) was born in 1945. He received the Dipl.Ing. degree in geodetic engineering in 1967 and the Dr.Tech. degree in 1972, both from the Technical University, Vienna, Austria.

He has worked at the International Institute for Aerial Surveys and Earth Sciences, Delft and Enschede, the Netherlands, from 1969 to 1974. From 1974 to 1976, he was a research associate at the Jet Propulsion Laboratory, Pasadena, CA. From 1976 to 1984, he held an appointment at the Technical University, Graz, Austria, as a Professor of Photogrammetry and Remote Sensing. Simultaneously, he was Director of the Research Institute for Image Processing and Computer Graphics, Graz Research Center, Graz, Austria. He currently works with Markhurd Corporation, Minneapolis, MN. (He has authored about 100 articles.

Dr. Leberl was recipient of the Otto von Gruber Gold Medal of the International Society for Photogrammetry and Remote Sensing in 1976.

Michael Kobrick (M'81) received the B.S. degree in physics from Rensselaer Polytechnic Institute, Troy, NY, the M.S. degree in astronomy from the University of Illinois and the M.S. and Ph.D. degree in planetary and space science from the University of California, Los Angeles.

A Research Scientist at the Jet Propulsion Laboratory, Pasadena, CA, his current research interests include radar remote sensing of planetary surfaces and, in particular, the derivation and geophysical analysis of topographic information. He is the Science Manager of the Venus Radar Mapper project, a Principal Investigator on the Shuttle Imaging Radar, Coinvestigator in the development of a new high-frequency radar altimeter for the Mars Geoscience and Climatology Orbiter, and Principal Investigator of the Digital Topographic Mapping Mission study project.

Dr. Kobrick is a member of the American Astronomical Society, Divisions for Planetary Science and Dynamical Astronomy, American Geophysical Union, AAAS, Sigma Xi American Institute of Physics, Astronomical Society of the Pacific, and the American Society of Photogrammetry, and has served on several NASA advisory panels for planetary radar as well as the Federal Interagency Coordinating Committee for Digital Cartography.



Johannes Raggam received the Dipl.Ing. degree in geodetic engineering from the Technical University, Graz, Austria, in 1980. He is currently working toward the Ph.D. degree on the subject of stereo radar at the Research Institute for Image Processing and Computer Graphics of the Graz Research Center, Graz, Austria.

As part of his work, he developed a capability to employ a photogrammetric computer controlled stereo instrument with overlapping side-looking radar images.